JGR Atmospheres

RESEARCH ARTICLE
10.1029/2019JD031772

Climate State Dependence of Arctic Precipitation Variability

L. Bogerd[1,2], E. C. van der Linden[1,3], F. Krikken[1], and R. Bintanja[1,4]

[1]Royal Netherlands Meteorological Institute, De Bilt, Netherlands, [2]Institute for Marine and Atmospheric research Utrecht, Utrecht, Netherlands, [3]Water Systems and Global Change Group, Wageningen University and Research, Wageningen, Netherlands, [4]Energy and Sustainability Research Institute Groningen (ESRIG), University of Groningen, Groningen, Netherlands

Key Points:
- Increase in precipitation variability does not scale with increase in mean precipitation toward warmer climates
- Increase in mean evaporation toward warmer climates is important for increase in mean precipitation during winter
- Variability in poleward moisture transport is the main source for precipitation variability in both seasons and across all climate states

Supporting Information:
- Supporting Information S1

Correspondence to:
R. Bintanja,
r.bintanja@rug.nl

Citation:
Bogerd, L., van der Linden, E. C., Krikken, F., & Bintanja, R. (2020). Climate state dependence of Arctic precipitation variability. *Journal of Geophysical Research: Atmospheres*, *125*, e2019JD031772. https://doi.org/10.1029/2019JD031772

Received 4 OCT 2019
Accepted 26 MAR 2020
Accepted article online 4 APR 2020

Author Contributions:
Conceptualization: R. Bintanja
Formal analysis: L. Bogerd
Investigation: F. Krikken
Methodology: E. C. van der Linden, F. Krikken, R. Bintanja
Project administration: R. Bintanja
Resources: R. Bintanja
Software: L. Bogerd, F. Krikken
Supervision: E. C. van der Linden, F. Krikken, R. Bintanja
Visualization: L. Bogerd
Writing - original draft: L. Bogerd
Writing – review & editing: R. Bintanja

Abstract Arctic precipitation is projected to increase more rapidly than the global mean in warming climates. However, warming-induced changes in the variability of Arctic precipitation, which are related to surface evaporation and poleward moisture transport (PMT), are currently largely unknown. This study compares the precipitation variability in different quasi-equilibrium climates simulated by a global climate model (EC-Earth) and studies the underlying mechanisms. Five quasi-equilibrium simulations of 400 years length forced with a broad range of CO_2 concentrations (0.25, 0.5, 1, 2, and 4 times the current global mean) were analyzed. PMT is the dominant source of Arctic precipitation variability in colder climates when the ocean in the Arctic basin is completely covered by sea ice year-round. Arctic precipitation variability increases from colder to warmer climates, primarily in summer. In summer, the increasingly stronger relation between Arctic sea level pressure variability and precipitation variability toward warmer climates enhances variability. In winter, the severe increase in mean precipitation (due to enhanced evaporation) exerts a comparatively small increase in variability, and precipitation variability is modulated by both PMT and evaporation, which oppose each other as they both affect the vertical and meridional moisture gradients.

1. Introduction

Global warming will affect the Earth's hydrological cycle mainly because of the increasing moisture-holding capacity of the atmosphere. Hydrological changes can severely affect the living environment of people and animals, in one instance because the risk of floods increases due to more frequent and intense rainfall (Hassol & Corell, 2006; IPCC, 2013). A proper understanding of the changes in the hydrological cycle in a warmer climate is therefore crucial for assessing future climate impacts.

While climate warming will change precipitation rates over large parts of the globe, the increases in the Arctic region are projected to be particularly severe. The increase in precipitation in the Arctic region is relatively large (4.5% K^{-1}) compared to the global value of ~2% K^{-1} (Held & Soden, 2006). This strong increase can be attributed mainly to sea ice retreat, causing enhanced surface evaporation (Bintanja & Selten, 2014), with the increased poleward moisture transport playing a secondary role. In addition, the moisture holding capacity of the Arctic atmosphere increases relatively quickly because the Arctic region warms more strongly than other parts of the world (i.e., Arctic amplification) due mainly to local feedbacks (Manabe & Stouffer, 1980; Serreze & Francis, 2006).

Freshening of the Arctic ocean, due to increased Arctic precipitation, ice melt, and enhanced continental runoff, might affect the source regions of deep water formation as well as the strength of the Atlantic Meridional Overturning Circulation (AMOC) (Bintanja & Selten, 2014), which can modulate the climate in Europe (Haarsma et al., 2015; AMAP, 2012) and beyond. Also, the increase in atmospheric moisture amplifies polar warming by reinforcing water vapor and cloud feedbacks (Eastman & Warren, 2010; Vavrus & Harrison, 2003). Hence, it is of importance to investigate the hydrological cycle in this region in more depth, as changes in the Arctic may have regional as well as wide-ranging effects.

Most research on the changing hydrological cycle has focused on assessing trends in mean quantities. However, strong temporal variations can occur on interannual and decadal time scales, especially in the Arctic, which can temporarily obscure or enhance long-term trends (Hawkins & Sutton, 2009; Screen

et al., 2014). Increased knowledge about the (potentially changing) frequency and magnitude of climate variability, as well as the underlying processes, will thus help interpret climate trends. Moreover, interannual variability of the hydrological cycle is one of the governing aspects of precipitation extremes (Pendergrass et al., 2017) and hence hydrological impacts.

Internal climate variability in the Arctic is mainly associated with large-scale atmospheric circulation systems. In the Arctic region, the Arctic Oscillation (AO) is the dominant mode of variability and in terms of circulation regimes strongly linked to precipitation variability (Boer et al., 2001; Groves & Francis, 2002; Oshima & Yamazaki, 2004). The relation between atmospheric circulation regimes and temperature variability will alter toward warmer climates because of the diminishing role of sea ice due to melting (Reusen et al., 2019; Van der Linden et al., 2017).

Variability in the meridional moisture gradient can alter the Arctic's hydrological variability by affecting poleward moisture transport (PMT) originated from the subpolar and midlatitudes. Additionally, precipitation variability is locally affected by the availability of open water. In warmer conditions, interannual sea ice variability will decrease (Reusen et al., 2019), which is expected to affect variability in the amount of atmospheric moisture in the Arctic through surface evaporation. How such changes will combine to affect precipitation variability is, however, not yet understood. Also, the manner through which changes in Arctic precipitation variability scale with changes in the mean values is unclear, since these may be governed by different processes.

This study will identify climate mechanisms that govern the variability of the Arctic's hydrological cycle (with the main focus on precipitation variability) by evaluating model-simulated climate response to different concentrations of atmospheric CO_2. Four long climate simulations representing two colder and two warmer than present quasi-equilibrium climates will be used to elucidate differences in precipitation, evaporation and PMT variability between climate states, and changes in the means. This paper will discuss processes that contribute to changes in the hydrological cycle, especially temporal variability, which helps to quantify and interpret future changes in climate extremes in the Arctic, as well as their potential impacts.

2. Methods

2.1. Model and Simulations

2.1.1. Global Climate Model

Data sets of long duration (e.g., centuries) are arguably the most appropriate way to study (decadal) climate variability. Unfortunately, reanalyses and observations are not available over sufficiently long time periods. Moreover, observations in the Arctic are sparse and commonly exhibit long-term forced trends. Therefore, we will use long quasi-equilibrium simulations of a state-of-the-art fully coupled global climate model (GCM) to assess climate variability. We will use the EC-Earth model, version 2.3 (Hazeleger et al., 2012), which was applied in the Coupled Model Intercomparison Project Phase 5 (CMIP5) (Taylor et al., 2012).

In EC-Earth, the atmospheric, oceanic, sea ice, and land surface components are coupled by the Ocean, Atmosphere, Sea Ice, Soil coupling module (OASIS) (Valcke et al., 2003). The Integrated Forecast System (IFS) of the European Center for Medium-range Weather Forecasts (ECMWF) for the atmospheric component runs at T159 spectral resolution with a vertical resolution of 62 height levels. The Nucleus for European Modeling of the Ocean (NEMO) model for the ocean uses a horizontal grid configuration with a resolution of approximately 1.1° and a vertical resolution of 42 levels. The performance of the EC-Earth model in the Arctic in terms of the mean and variability (e.g., AO) can be found in Koenigk et al. (2013) and Reusen et al. (2019), respectively. The Arctic's oceanic components are evaluated by Koenigk and Brodeau (2014) and Sterl et al. (2012). The EC-Earth model realistically simulates various aspects of the global climate (Hazeleger et al., 2012), the atmospheric dynamics that govern poleward energy transport (sensible and latent heat) (Reusen et al., 2019) and surface evaporation (Koenigk et al., 2013).

Equilibrium climate states are appropriate to analyze climate variability because any forced component that influences the variability is thus eliminated. Therefore, five simulations with fixed CO_2 concentrations (multiplications of 0.25, 0.5, 1, 2, and 4 compared to the present-day CO_2 concentration, Van der Linden

et al., 2017) were carried out. First, the initial state of the control climate was obtained from a spin-up of a preindustrial climate simulation over about 1,000 years, after which an integration with present-day forcing (including greenhouse gas and aerosol concentrations, land use, and solar insolation equivalent to the year 2000) was carried out over 44 years. After this period, the five constant CO_2 concentrations were applied instantaneously, after which the integrations continued for another 550 years for each CO_2 forcing (Van der Linden et al., 2019). The upper ocean layers are assumed to be in quasi-equilibrium after 150 years (Van der Linden et al., 2019); hence, here we only use the final 400 years of the simulations.

2.1.2. Evaluation With Reanalyses Data

To evaluate the performance of the EC-earth model in the Arctic, the control simulation with present-day conditions and forcing was compared to reanalysis data (NASA MERRA-2 (Gelaro et al., 2017), ERA-Interim (Dee et al., 2011), and NCEP/CFSR (Saha et al., 2010)). Because of the large observational uncertainties in the Arctic region, and the relatively short time period (especially for decadal variability), a multireanalyses mean is expected to yield the most accurate "observations" for model evaluation. In addition, using multiple reanalyses provides an "observational" uncertainty estimate. Hence, we took the average of the three reanalysis data sets (both in the mean and in variability) and compared values from the period 1981–2010 (being representative for the present-day climate) with those from the EC-Earth control simulation in section 3.1.

2.2. Components in the Arctic Moisture Budget

The Arctic region is defined as the area 70–90°N (Groves & Francis, 2002; Oshima & Yamazaki, 2004; Sorteberg & Walsh, 2008). Only monthly mean model output (calculated from 1 hr model time steps) was available for this study. The following model variables were used in the analyses: total precipitation (TP) (convective + large-scale precipitation), specific humidity, surface evaporation (E), sea level pressure, geopotential height, sea surface temperature, and sea ice concentration. Other climate variables were calculated as specified below.

2.2.1. Total Precipitable Water

Specific humidity (kg kg^{-1}) (q) was converted and integrated over height to total precipitable water (mm) (Q). The integration was performed from 1,000 to 20 hPa over 16 height intervals (the moisture concentration was negligible above 20 hPa). The integration was performed with the trapezoidal method (following Dufour et al., 2016):

$$Q = \frac{-1}{g}\int_{surface}^{top} q\,dp = \frac{\sum_{surface}^{top}(q_n + q_{n+1})*(p_n - p_{n+1})}{2*g}$$

with g the gravitational acceleration and p the pressure level.

2.2.2. PMT Toward the Arctic

Meridional moisture transport ∇qv is usually calculated by evaluating the three-dimensional moisture and velocity fields along a latitude circle. However, over sufficiently long-time intervals (e.g., seasonal and annual), the water balance method is quite accurate (Bengtsson et al., 2011), especially when the atmospheric storage term is included (Dufour et al., 2016). Hence, the seasonal moisture transport into the Arctic (70–90°N) through 70°N was estimated from the following relation (Bengtsson et al., 2011; Groves & Francis, 2002):

$$-\nabla qv = TP - E + \frac{\partial Q}{\partial t}$$

where the $\partial Q/\partial t$ term was calculated using central differences between monthly values. As temperature rises, the $\partial Q/\partial t$ term (the tendency of precipitable water) is expected to become more important owing to the exponential (Clausius-Clapeyron) relation between specific humidity and temperature.

2.2.3. Geostrophic Wind at 500 hPa

The geopotential height (Φ) at 500 hPa can be used as proxy for the jet stream (e.g., Francis & Vavrus, 2015). We will use the geostrophic wind ($\vec{v}_g$), which was calculated as follows:

$$u = \frac{-g}{f^* r}\frac{\partial \Phi}{\partial \varphi}$$

$$v = \frac{g}{f^* r^* \cos(\varphi)}\frac{\partial \Phi}{\partial \lambda}$$

$$\overrightarrow{v}_g = \sqrt{u^2 + v^2}$$

where u and v are, respectively, the zonal and meridional wind components, f the Coriolis parameter (defined as $f = 2\ \Omega \sin \varphi$ with Ω (7.2921×10^{-5} rad s^{-1}) the rotation of the Earth), λ the longitude, φ the latitude, and r the radius of the Earth.

2.2.4. Arctic Oscillation (AO)

Multiple studies have shown a relationship between the AO and meridional moisture transport (Groves & Francis, 2002; Jakobson & Vihma, 2010; Oshima & Yamazaki, 2004). Because the AO is linked to the polar vortex, thereby influencing the variability in lower-tropospheric winds which are important for meridional moisture transport (Groves & Francis, 2002), it alters precipitation variability. In current climate, a positive AO index is associated with warmer conditions and a strengthened atmospheric circulation over the Arctic. Through the strengthened circulation, more moisture is being advected toward the Arctic (Oshima & Yamazaki, 2004), which increases the amount of precipitation in the Arctic region. Therefore, it is vital to analyze the AO index, in particular because the AO index may become more positive in warmer climates (Gillett, 2002; Rind et al., 2005).

The AO is the hemispheric expression of the dominant sea level pressure pattern associated with climate variability over the region 20–90°N (Thompson & Wallace, 1998). The strength of the AO is measured by the AO index which is defined as the magnitude of the principle component of the first empirical orthogonal function (EOF) of sea level pressure. The strength of the AO is most pronounced in winter (Boer et al., 2001; Jakobson & Vihma, 2010), but the AO is potentially more important in summer due to the abundance of atmospheric moisture (Groves & Francis, 2002).

2.3. Analyses

2.3.1. Interannual and Decadal

Temporal variability on shorter (interannual) time scales is linked to other mechanisms than those that govern longer-term (decadal) variabilities. Interannual variations are generally associated with atmospheric processes, whereas decadal variations are often dominated by ocean interactions due to the ocean's comparatively high inertia and heat capacity (Reusen et al., 2019). To assess such differences, the time series were subdivided into high and low frequencies following Reusen et al. (2019). After the annual and seasonal averages were calculated, and the averaged data were linearly detrended in order to remove any remaining trend, a fourth-order Butterworth filter with a cutoff frequency of 0.1 $year^{-1}$ was applied. Henceforth, we subdivide variability into an interannual part (periodicity shorter than 10 years) and a decadal part (longer than 10 years). Changing the cutoff frequency did not qualitatively affect the results.

2.3.2. Seasonal Patterns

The present-day Arctic climate is characterized by distinct seasonal patterns in the hydrological cycle. In winter, the variability in the number and intensity of cyclones infiltrating the Arctic region is high compared to summer (Sorteberg & Walsh, 2008), which is linked to amplified PMT. Furthermore, wintertime evaporation is largest over the North Atlantic (Jakobson & Vihma, 2010), and the AO is most pronounced in winter (Groves & Francis, 2002; Thompson & Wallace, 1998). In summer, the moisture content of the atmosphere is highest (Groves & Francis, 2002). Because of the strong seasonality in hydrological variables and processes that are presumably important for Arctic hydroclimatic variability, we will focus mainly on winter (December, January, February [DJF]) and summer (June, July, August [JJA]) patterns and the differences between these seasons.

2.3.3. Variability

The standard deviation was used as a metric for the magnitude of variability, in line with previous studies on precipitation variability (Boer, 2009; Groves & Francis, 2002; Pendergrass et al., 2017). Relations between variables were examined by calculating regressions (which indicate the numerical impact of a change in the independent variable on the dependent variable) and correlations (which indicate how strong two variables are related). Spatial patterns of precipitation variability were quantified using EOF analysis.

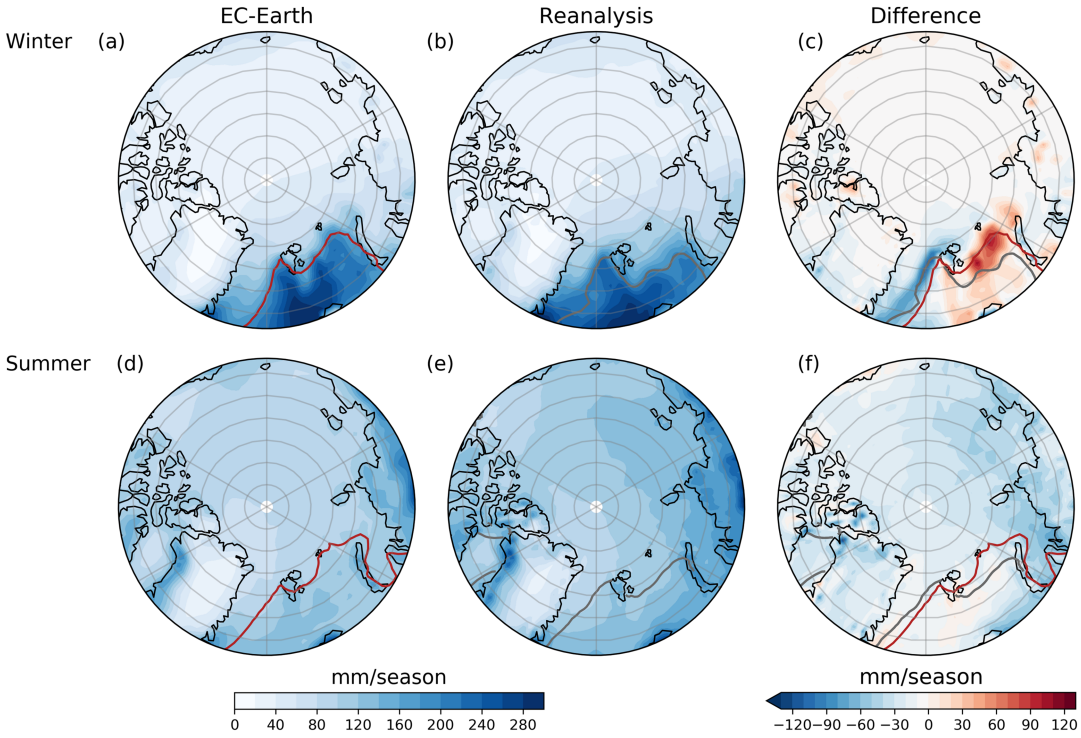

Figure 1. Mean precipitation for EC-Earth (control simulation), reanalyses, and its difference (EC-Earth minus reanalysis) for winter (a–c) and summer (d–f). The gray and red contours indicate the average 15% sea ice concentration isopleth in the reanalyses and model, respectively.

A measure of the uncertainty in the means and variability was provided by a bootstrap test (with 1,000 random samples) on the seasonally averaged and detrended time series. In this method, random data points are taken from the original data set (with replacement), of which a new sample is created. The associated 5th and 95th percentiles are used to indicate the uncertainties. The same method is used to determine significance levels in the differences between reanalyses and model-simulated variability: Differences are marked as significant if the respective uncertainty estimates do not overlap.

3. Results and Discussion

3.1. Precipitation Characteristics of the Arctic and Model Evaluation

3.1.1. Mean Precipitation

The average precipitation in both winter and summer for the EC-Earth control climate and the reanalyses is shown in Figure 1, together with the respective differences. The contours indicate the mean 15% sea ice concentration isopleth, an often-used indication of the sea ice margin (Deser et al., 2000; Zhang et al., 2013).

In general, precipitation decreases with increasing latitude and altitude because of lower air temperatures, limiting the moisture-holding capacity of the atmosphere. In winter, the highest precipitation rates are found over the North Atlantic (Figures 1a and 1b). This is due to vertical instabilities caused by the relativity warm open water but low air temperatures (Serreze & Hurst, 2000), inducing convection and moisture advection within the North Atlantic storm track (Dufour et al., 2016; Jakobson & Vihma, 2010). Over the Pacific side of the basin, previous studies found that the North Pacific storm track transports moisture into the Arctic basin (Groves & Francis, 2002; Sorteberg & Walsh, 2008), although the effect here is smaller compared to the Atlantic side of the Arctic.

In summer, precipitation is more zonally distributed (Figure 1d) which is related to (i) a relatively weak, low-pressure system over the Arctic Ocean (occurring in both the model simulation (Van der Linden et al., 2017; their Figure 5d) and the reanalyses (Groves & Francis, 2002; Oshima & Yamazaki, 2004)) that causes moisture to circulate counterclockwise over the Arctic, (ii) the higher air temperatures result in a

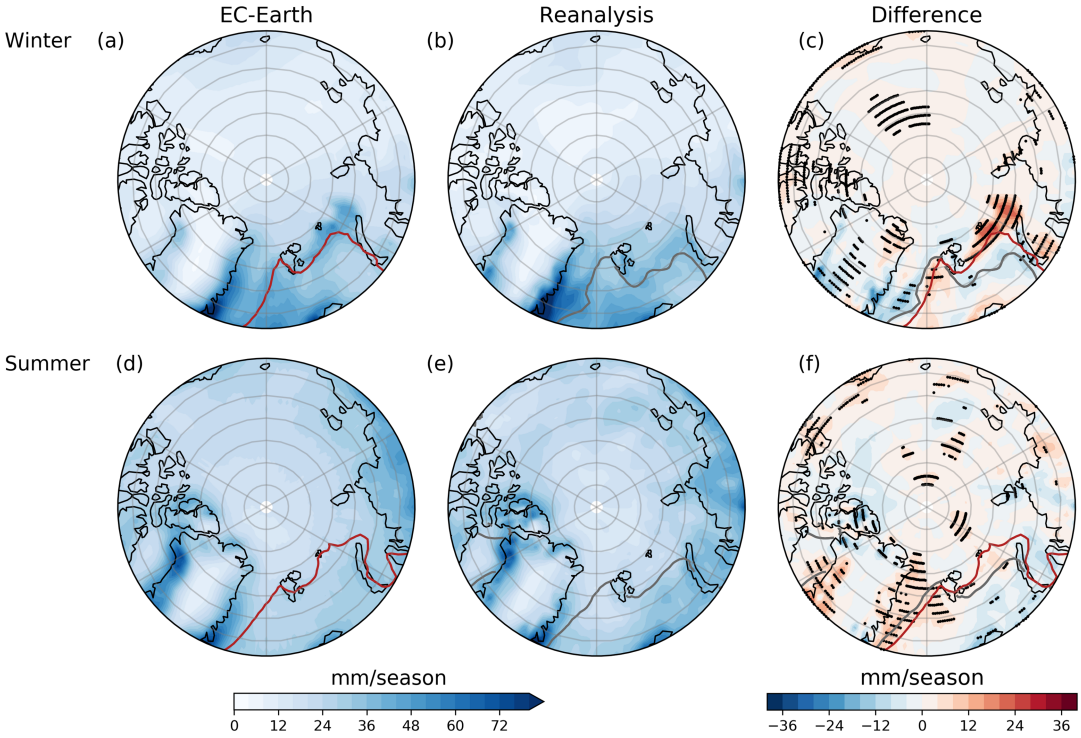

Figure 2. Similar as Figure 1 but now for precipitation variability. Differences are marked as significant (black dots) if the uncertainty estimates do not overlap.

more stable near-surface stratification over open water compared to winter (not shown) and smaller evaporation rates, and (iii) the North Atlantic storm track is weaker compared to winter (Groves & Francis, 2002), which reduces precipitation rates over the North Atlantic. There is also a relatively strong precipitation gradient over land-ocean boundaries (with higher values over land; Figure 1d) because of increased cyclogenesis over the continents (Serreze & Hurst, 2000) and a more unstable near-surface stratification over land compared to winter, as land is relatively warm compared to air transported from the (frozen) Arctic Ocean. Summed over the Arctic (both land and ocean), the total summertime precipitation rate is higher than in winter because the atmosphere can hold more moisture due to higher air temperatures.

The EC-Earth model is generally able to simulate Arctic precipitation rates fairly accurately, despite the systematic underestimation in summer (Figure 1f), especially compared to CSFR and MERRA-2. However, it should be mentioned that the CFSR and MERRA-2 generally produce relatively high Arctic precipitation rates compared to other reanalyses (e.g., Bintanja et al., 2020). In winter, two main regions can be distinguished where the model deviates from reanalyses: (i) The precipitation to the east of Svalbard is overestimated, and (ii) the precipitation to the east of Greenland is underestimated. Both are most likely caused by the difference in sea ice edge between the model and reanalyses since the ice margin in EC-Earth is located more to the northwest than in the reanalyses data (Figure 1c). Differences between EC-Earth and reanalyses are significant everywhere. This is because the detrending resulted in a relatively constant mean with only small fluctuations over time. The bootstrapping of the differences between the EC-Earth model and the reanalyses data thus resulted in significant differences for almost every grid point. However, except for the regions near the sea ice edge, the mean values in the control simulation were always between that of the lowest and the highest mean value of the three reanalysis data sets.

3.1.2. Precipitation Variability

The simulated and reanalyses precipitation variability is shown in Figure 2. During both winter and summer (Figures 2a and 2d), the pattern is roughly similar to that of the mean precipitation (Figures 1a and 1d, respectively). In winter, precipitation variability is highest over the North Atlantic (Figure 2a). This high variability is most likely caused by fluctuations in the sea ice margin. In addition, the passage of cyclones

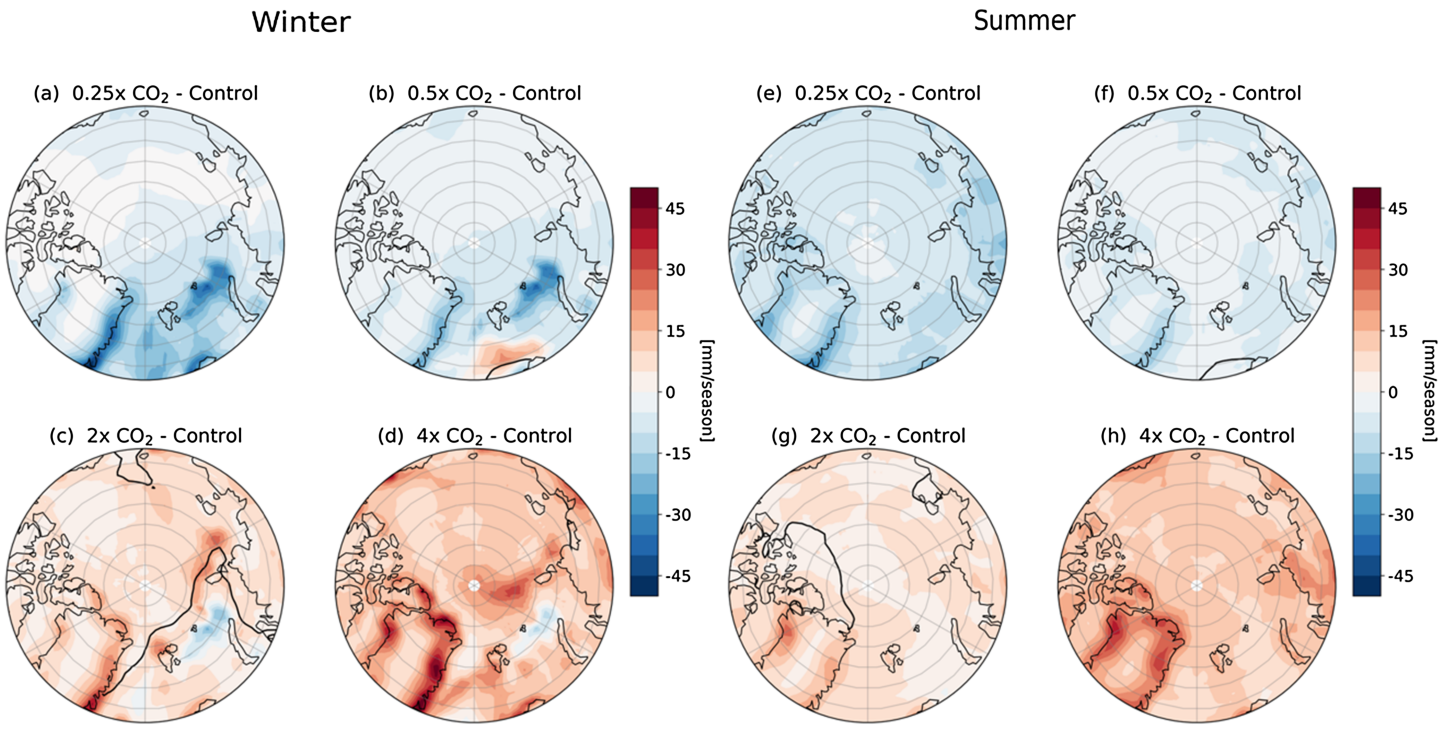

Figure 3. Precipitation variability of the four climate states relative to the control climate in winter (left, a–d) and summer (right, e–h). The black contour indicates the 15% sea ice concentration isopleth in each climate/season, which is not visible in the 0.25xCO2 (due to extreme southward sea ice expansion) and 4xCO2 (totally unfrozen Arctic Ocean) climates.

from the North Atlantic storm track and (to a lesser extent) from the Pacific storm track contributes to considerable fluctuations in PMT. The east of Greenland exhibits strong variability (Figure 2a), which in previous studies has been linked to the North Atlantic storm track (Groves & Francis, 2002; Sorteberg & Walsh, 2008).

In summer, the pattern of precipitation variability is roughly similar to the mean precipitation, that is, more zonally distributed over the Arctic (Figure 2d). The magnitude of variability is stronger than that in winter, especially in the central Arctic, probably because of the relatively high mean precipitation levels.

For both winter and summer (Figures 2a and 2d), high precipitation variability is observed near the margins of Greenland. This is due to orographic uplift caused by the high elevation of the ice sheet: As air is forced to rise, it cools adiabatically, resulting in condensation and precipitation. The high variability at the margins is then related to large-scale circulation patterns. For example, in positive (negative) AO during winter, the moisture is transported from the east (west) toward Greenland (Groves & Francis, 2002; their Figure 15), resulting in precipitation mainly on the eastern (western) side (Figure S1 in the supporting information) of the ice sheet.

In general, EC-Earth slightly overestimates precipitation variability during winter (Figure 2c), especially over regions with low variability (an overestimation in the range of 0–4 mm per season over the Arctic Ocean and Canadian Archipelago). In summer, the differences between the simulation and reanalyses are more spatially scattered (Figure 2f). The difference in variability between EC-Earth and reanalyses exhibits a similar pattern as in mean precipitation, with the largest deviations being related to the difference in sea ice edge location in winter. Otherwise, regions where the differences are significantly different are comparatively small. We therefore conclude that, apart from some regional deviations, EC-Earth is able to accurately simulate precipitation characteristics (means and variability) of the current climate.

3.2. Precipitation Variability in Different Climate States

The difference in precipitation variability between climate states (relative to the control climate) is shown in Figure 3. Evidently, the total precipitation variability in both seasons increases toward warmer climates (the

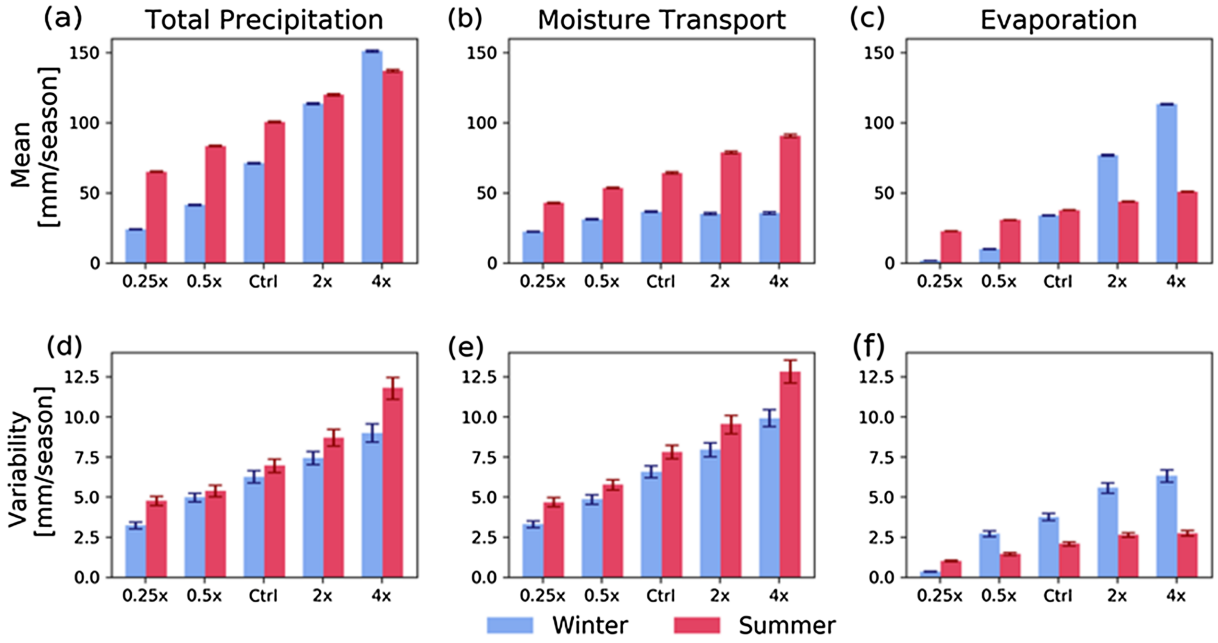

Figure 4. Arctic means (a–c) and variability (d–f) of total precipitation, PMT, and evaporation in winter (blue) and summer (red) for the five climate states (means over 70–90°N). Error bars for variability indicate the 5th and 95th percentiles uncertainty.

bottom row of Figure 3). Both seasons exhibit a large increase (decrease) of precipitation variability near the margin of Greenland in warmer (colder) climates. We will focus on the regions within the Arctic with the largest (changes in) variability.

The increase of precipitation variability near the Greenland coast may follow the already observed trend in the mean (Mernild et al., 2015) and can be attributed to a combination of both atmospheric moisture availability and the altered passage of cyclones (Schuenemann & Cassano, 2010). Because precipitable water increases in warmer climates, more precipitation is forced to fall when the air cools adiabatically as it is pushed upward onto the Greenland Ice Sheet. The opposite happens in colder climates, as less moisture is available due to lower temperatures and greater sea ice extent (inhibiting surface evaporation).

Interestingly, the region north of the Barents Sea exhibits reduced variability for both colder (Figures 3a and 3b) and warmer (Figures 3c and 3d) climates in winter. In the control simulation, the sea ice edge is located in this region, resulting in precipitation variability due to fluctuations in the sea ice edge. In warmer climates, sea ice retreats northward (which affects surface evaporation) and the inflow of warm ocean water is enhanced (which influences the vertical temperature gradient in the lower atmosphere (Van der Linden et al., 2016; Van der Linden et al., 2019), resulting in larger variability in evaporation values (Figure S2)). Therefore, the variability in precipitation that follows the sea ice edge is shifted northward as well. In colder climates, the opposite situation occurs (Figures 3a and 3b) as the sea ice expands southward (where variability increases) and the influx of warm ocean water is reduced (resulting in reduced evaporation variability, Figures S2a and S2b).

In summer, the variability increase (decrease) toward warmer (colder) climates is more spatially uniform over the ocean, as higher air temperatures in comparison to the winter season reduce the vertical temperature gradients over the open water, thereby increasing atmospheric stability. The patterns of change in precipitation variability across climate states are quite similar between states. The magnitude of variability, however, is amplified, especially toward warmer climates. For instance, the increase in precipitation variability compared to the control climate is more than twice as large for the $4xCO_2$ climate (Figure 3h) than for the $2xCO_2$ climate (Figure 3g).

Compared to winter, changes in precipitation variability in summer toward warmer climates are more pronounced over the continents. A possible explanation may be found in the occurrence of cyclones, which

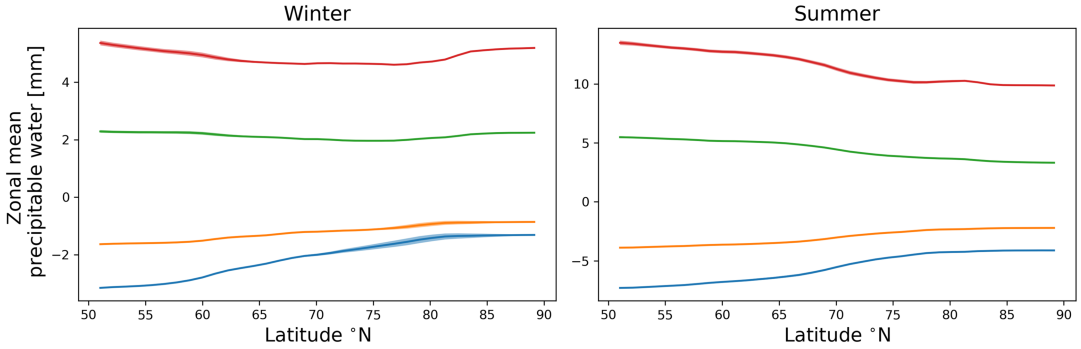

Figure 5. Difference in vertically integrated precipitable water between the various climate states and the control climate in (left) winter and (right) summer. The shading indicates the standard deviation (also relative to the control climate).

contribute to precipitation variability. Currently, trends seem to hint toward winter cyclones being more intensified over the ocean, whereas the increase in summer cyclones is more focused over the continents (Tilinina et al., 2013).

To obtain further insights into the mechanisms behind changes in precipitation (means and variability), it is helpful to study the various components of the Arctic's hydrological cycle in the atmosphere. To this end, the Arctic mean and variability of total precipitation, PMT across 70°N, and surface evaporation are shown in Figure 4.

3.2.1. Changes in the Mean State

Total precipitation is lowest in both seasons for the coldest climate and steadily increases toward warmer climates. The total Arctic precipitation is (with the exception of the 4xCO_2 climate) lower in winter than in summer. In winter, the increase in total precipitation is predominantly driven by the increase in evaporation (Figure 4c), in agreement with Bintanja and Selten (2014) and Dufour et al. (2016) (the latter attributes the observed increase in specific humidity over the past 30 years to evaporation). Surface evaporation increases toward warmer climates because of the retreating sea ice and also the intrusion of relatively warm ocean water into the Arctic, resulting in enhanced energy exchange between the ocean and atmosphere through surface evaporation.

PMT through 70°N originates from southerly regions, where the atmosphere contains more moisture compared to the Arctic, due to higher ambient temperatures. Owing to the nonlinearity of the Clausius Clapeyron equation, the increase in moisture per degree warming toward warmer climates is higher at more southern latitudes. However, this is partly offset by Arctic amplification (which is strongest in winter (Koenigk et al., 2013; Screen & Simmonds, 2010)) and the related increase in Arctic evaporation. The differences in the zonal mean of precipitable water (integrated over height) of the various climate states with the control climate are shown in Figure 5 which shows that, especially in winter, the meridional moisture gradient remains fairly constant toward warmer climates.

In summer, the increase in total precipitation toward warmer climates seems to be governed by enhanced PMT (Figure 4b). The warming-induced increase in vertically integrated precipitable water is amplified in the southern latitudes (Figure 5, right) as Arctic amplification is less pronounced in summer. Therefore, the meridional moisture and temperature gradients increase toward warmer climates, which tends to enhance the moisture transport toward the Arctic. The evaporation increases only slightly (Figure 4c) because higher air temperatures result in a more stable stratification of the boundary layer over the Arctic Ocean (which is further elaborated on in section 3.5).

3.2.2. Changes in Variability

For all variables and both seasons, the Arctic mean precipitation variability increases from cold to warm climates (Figure 4d). For all climate states, the variability in total precipitation is (slightly) higher in summer than in winter, whereas the changes in mean precipitation are stronger in winter. The relatively small change in wintertime precipitation variability toward warmer climates compared to the change in mean precipitation is in agreement with the findings of Pendergrass et al. (2017).

Interestingly, the variability of PMT increases in winter (Figure 4e), even though its mean value is relatively constant across the various climates. This suggests that changes in the variability of the Arctic hydrological cycle do not simply scale with changes in the mean atmospheric moisture values, implying that other climate mechanisms (such as changes in atmospheric circulation) also contribute to the changes in variability.

The various components of the Arctic's hydrological cycle (Figure 4) exhibit three interesting trends that will be evaluated in more detail in the next sections: (i) The variability in wintertime PMT increases with warming, while the mean remains relatively constant, (ii) the increase in precipitation variability is relatively small compared to the increase in mean precipitation, and (iii) the variability in precipitation is higher in summer than in winter.

3.3. PMT in Winter

Figure 4b shows that the mean PMT in winter is relatively constant among the various climate states (as discussed in section 3.2), while its variability steadily increases toward warmer climates. Figure 5 shows that the precipitable water content increases toward warmer climates (in both the Arctic and the midlatitudes). Hence, even though the wintertime PMT remains roughly constant between the various climates (Figure 4b), the total amount of atmospheric moisture increases.

Generally, apart from the availability of atmospheric moisture, the mean and variability in PMT are affected by atmospheric circulation processes, such as the intensity and number of cyclones (the dynamical component of PMT will be discussed in more detail in the next sections). Before a cyclone enters the Arctic, in warmer climates, it will take up relatively high amounts of moisture due to the higher atmospheric moisture content. The corresponding moisture transport will thus strongly enhance the precipitable water content in the Arctic, especially in the warmest climates.

Our results show that the correlation between PMT and Arctic sea level pressure variability is relatively constant toward warmer climate states during winter ($r = -0.59$, $r = -0.56$, and $r = -0.58$ for the control, $2xCO_2$ and $4xCO_2$, respectively). Also, the position of the winter North Atlantic jet stream (which is strongly linked to the position of the storm track) does not change much between the various climates (not shown).

In summary, while the mean PMT is relatively constant due to compensating mechanisms linked to reinforced Arctic warming and the nonlinearity of the Clausius-Clapeyron relation, its variability is enhanced toward warmer climates which is most likely due to higher atmospheric moisture content especially near the locations of maximum cyclonic activity near 70°N.

3.4. The Influence of Evaporation and PMT on Precipitation Variability During Winter

Figure 4 also shows that the increase of total precipitation variability toward warmer climates is relatively small compared to the increase in mean precipitation, which has a direct effect on the variability. We expect that evaporation and PMT oppose each other, because both components influence the atmospheric vertical moisture gradient. To confirm this hypothesis, the mutual relations between variability in precipitation, PMT, and evaporation will be analyzed in terms of their phase and governing mechanisms. Additionally, the time scale of the variability will be considered, since it is expected that the processes governing variability on shorter time scales will be different from those on longer time scales (as mentioned in section 2.3.3). Separating between short and long time scales may provide insight in the causes of the spatial patterns in Figure 3.

It is expected that evaporation variability acts primarily on decadal time scales since it is primarily linked to the sea surface temperatures and ocean processes. Due to the large heat capacity of the ocean, atmosphere-ocean interactions induce low-frequency fluctuations in the surface fluxes (Van der Linden et al., 2016). Hence, it is expected that the correlations between evaporation and sea surface temperature on decadal time scales are relatively large compared to those on interannual time scales.

Except for the $0.25xCO_2$ ($r = 0.53$) and $0.5xCO_2$ ($r = 0.79$) climates, evaporation and sea surface temperature exhibit correlations smaller than |0.34| on interannual time scales. Decadal variability exhibits stronger correlations for the $0.5xCO_2$ ($r = 0.93$), control, and $2xCO_2$ (both $r = 0.78$) climates. The relative low correlation for the $0.25xCO_2$ ($r = 0.42$) and $4xCO_2$ ($r = 0.22$) climates is most likely due to a lack of open water in the coldest climate and the absence of sea ice in the warmest climate. This indeed emphasizes that evaporation is linked to oceanic processes and that evaporation is more dominant on decadal time scales.

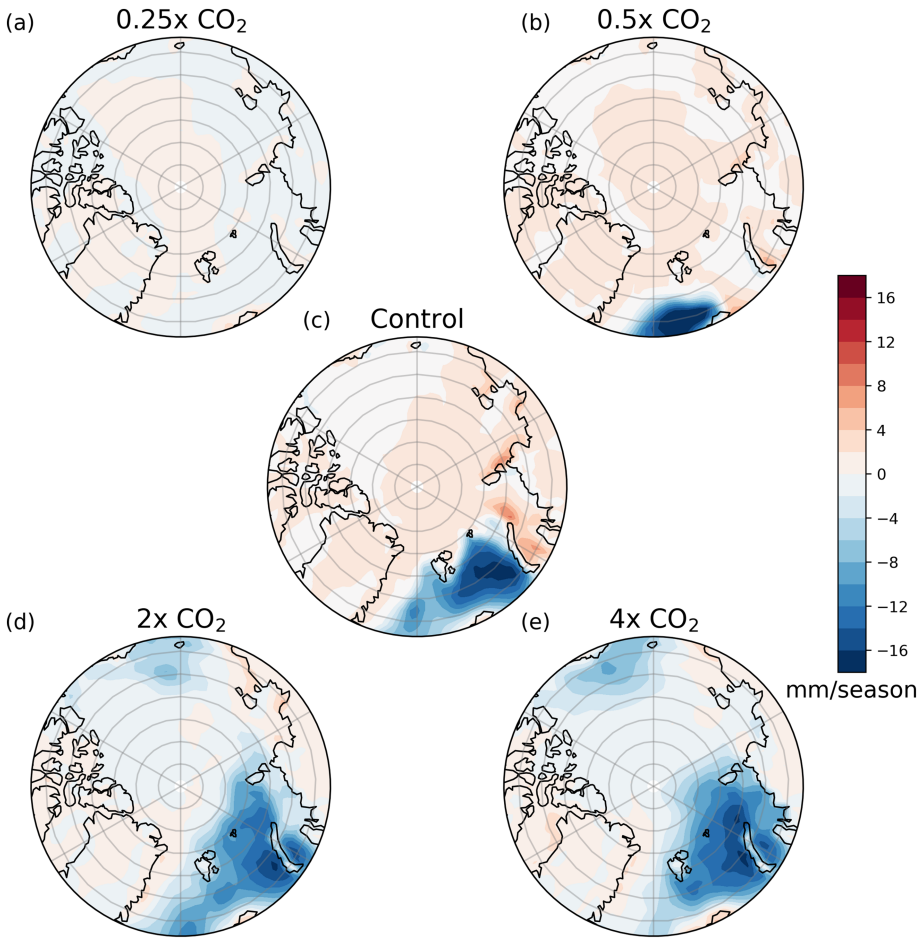

Figure 6. (a–e) Regression maps (70–90°N) of surface evaporation on the standardized PMT (the time series of poleward moisture transport anomalies is divided by its standard deviation) across 70°N in winter for interannual variabilities. Note that the scaling of Figures 6 and 7 is different.

In contrast, mechanisms associated with atmospheric moisture transport are expected to dominate interannual variability, as atmospheric processes act on relatively short time scales. To assess the time scale dependence of the processes governing precipitation variability and to evaluate whether increased PMT indeed causes reduced evaporation, regression maps between surface evaporation and the standardized PMT are shown in Figures 6 and 7 for interannual and decadal variabilities, respectively.

Negative regressions depicted in Figures 6 and 7 can be interpreted as follows: When moist air enters the Arctic, the vertical moisture gradient between the ocean and the atmosphere decreases, which in turn slows down evaporation (depending to a certain extent on atmospheric stability). On the other hand, if evaporation is enhanced, atmospheric moisture in the Arctic region increases which decreases the meridional moisture gradient, thereby reducing the PMT by eddies.

The interannual variability regressions show that the highest absolute values are found over areas where the sea ice permanently retreats. This occurs over the North Atlantic (in the $0.5xCO_2$ climate (Figure 6b)), and this region moves northward and eastward toward warmer climates. However, the variability in sea surface temperature (i.e., ocean heat transport) does not exhibit a similar spatial pattern (not shown), which strongly suggests that ocean heat transport is not the driver of interannual variability in evaporation over these regions.

Additionally, surface evaporation and Arctic precipitable water exhibit a negative correlation for interannual variability ($r = -0.42$ for the $0.25xCO_2$ climate, $r = -0.53$ for the control climate, and $r = -0.73$ for the $4xCO_2$ climate) averaged over the Arctic. This indicates that when Arctic atmospheric precipitable

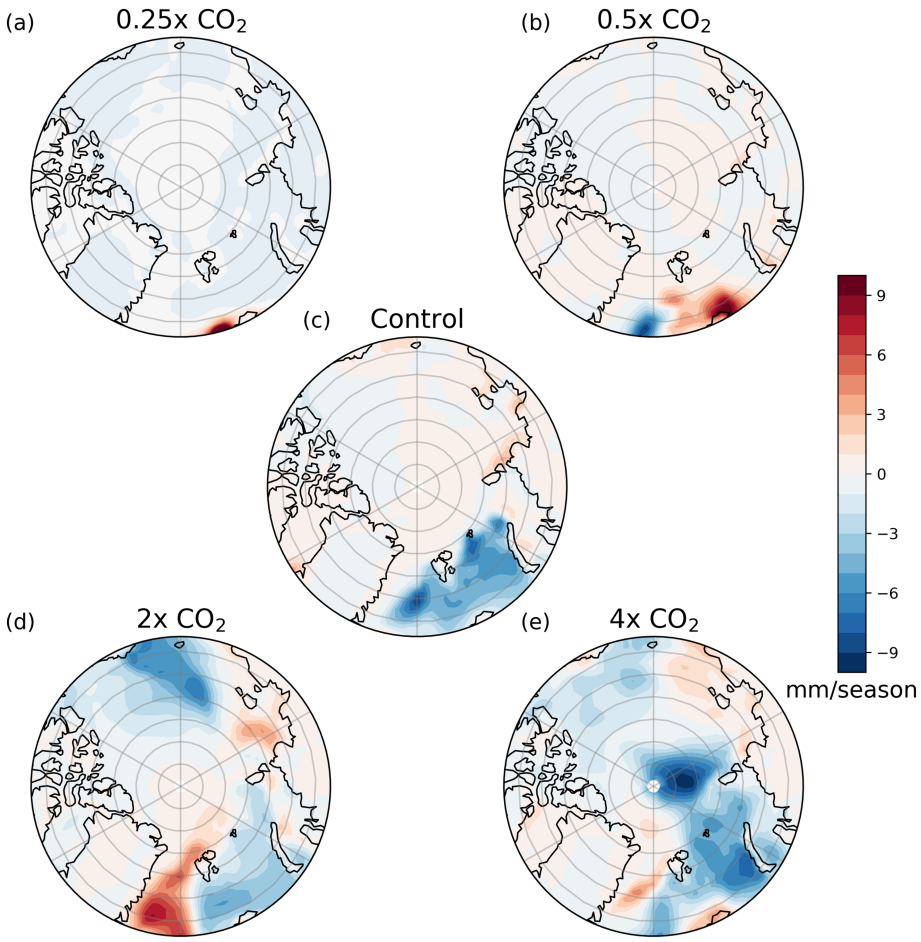

Figure 7. Similar as Figure 6 but now for decadal variability. Note that the scaling of Figures 6 and 7 is different.

water content is high, evaporation is reduced. In contrast, lower precipitable water contents are related to high evaporation values. Therefore, this negative correlation suggests that the interannual variability in precipitable water (and consequently, evaporation and precipitation) will most likely be determined by PMT, although causal relationships cannot be deduced from correlations.

The decadal variability (Figure 7) is, in contrast to the interannual variability, mainly apparent in regions where the sea surface temperature exhibits decadal variability (Figure S3). In the absence of sea ice, warmer ocean water enhances atmospheric instability over open oceans in winter. This reinforces turbulent fluxes (increasing surface evaporation), through which the amount of moisture in the atmosphere increases. Therefore, precipitable water and evaporation exhibit positive correlation values over the areas of decadal sea surface temperature fluctuations (while the correlation was negative for interannual variabilities).

This higher atmospheric water content opposes PMT through decreasing the meridional moisture gradient, resulting in negative regression values between evaporation and PMT (Figure 7). The decadal variability slightly decreases once sea ice has disappeared and decadal variability associated with the influx of warm ocean water is displaced further northward (Van der Linden et al., 2017).

For decadal variability, areas of strongly positive regression values can be observed in the North Atlantic (e.g., in the 0.5xCO_2 and 2xCO_2 climates). For these regions, increases in evaporation due to sea surface temperature fluctuations result in a positive regression with the PMT. Two explanations that may result in positive regressions between evaporation and PMT are put forward. First, positive regressions may be caused by our definition of PMT: a zonal average along the 70°N latitude circle, meaning that longitudinal variations are averaged out. Hence, even if the zonally averaged PMT increases, the moisture transport does not necessarily increase along all longitudes.

Second, the positive regressions may be caused by the dynamical components determining the PMT (e.g., pressure systems, wind direction) instead of thermodynamic interactions (i.e., moisture availability), which was the focus in the discussion about the relation between PMT and evaporation. In the $2xCO_2$ climate, strong positive regressions are found close to Greenland (Figure 7d). Schuenemann and Cassano (2010) suggested that increased atmospheric moisture due to enhanced evaporation over the Greenland Sea is transported through cyclones (associated with low-pressure systems) to the east coast of Greenland. Hence, this would mean that evaporation and moisture transport close to the coast of Greenland reinforce each other, resulting in positive regressions.

To summarize, precipitation variability is influenced by the interaction between PMT and evaporation since both influence the meridional moisture gradient in winter. When a distinction is made between interannual and decadal variabilities in atmospheric moisture, evaporation always exhibits a negative correlation for interannual variabilities, while decadal variabilities are indicated by positive correlations over regions where the sea surface temperature fluctuates. Therefore, in combination with the results above, we conclude that interannual precipitation variability in the Arctic is predominantly controlled by PMT, whereas decadal variability is predominantly controlled by Arctic surface evaporation.

3.5. Higher Summer Variability Compared to Winter

Figure 4d shows that, relatively speaking, the increase in total precipitation variability from cold to warm climates is stronger in summer than in winter. In the previous section, we elucidated the role of the interactions between evaporation and PMT in winter and thereby argued why the increase in wintertime precipitation variability is relatively small.

In summer, PMT and surface evaporation also exhibit a negative correlation, but the regressions are much weaker (not shown). The lower regression values are expected to be caused by the higher air temperatures due to incoming solar radiation, resulting in smaller vertical temperature gradients (and therefore moisture gradients) between the ocean and atmosphere (e.g., a more stable stratification of the atmospheric boundary layer over the Arctic Ocean). A smaller vertical gradient reduces the energy transfer between the ocean and the atmosphere (via turbulent fluxes), resulting in relatively low evaporation values.

To verify whether stability over the oceans is indeed stronger in summer, we analyzed the components of the total precipitation (i.e., convective and large-scale) separately. The first is associated mainly with local-scale vertical instabilities (e.g., fluctuations in vertical gradients), while the second is associated with large-scale dynamics (e.g., moisture convergence and orographic uplift). Therefore, it would be expected that wintertime surface evaporation is positively correlated with convective precipitation, whereas it should be negatively correlated with large-scale precipitation (since this is associated with reduced PMT, as explained in the previous paragraph). The correlations between convective and large-scale precipitation and with surface evaporation for both seasons are shown in Table 1.

The correlation between convective and large-scale precipitation decreases toward warmer climates in winter but remains roughly constant in summer. Table 1 verifies that in winter, except for the coldest climate (in which the ocean is completely frozen and the correlation with PMT is strongest), convective precipitation and evaporation exhibit a strong positive correlation, while the correlation between large-scale precipitation and evaporation becomes increasingly negative for warmer climates. This indicates that winters with relatively high large-scale precipitation (due to enhanced PMT), convective precipitation is reduced. As a consequence of the enhanced transport of relatively warm and moist air into the Arctic, the atmospheric instability and evaporation over the oceans are reduced, resulting in less convective precipitation in winter.

In summer, however, both large-scale and convective precipitation are not strongly correlated with evaporation. Due to the ice-free and warmer ocean, convective precipitation is reduced over the ocean (in agreement with Serreze & Hurst, 2000) and therefore shows a decreasing and even insignificant correlation with evaporation toward warmer climates. Convective precipitation is then more localized over land and is more dependent on the PMT. Because large-scale and convective precipitation are both related to PMT during summer, both contribute to precipitation variability, thereby increasing its magnitude. This subdivision in precipitation types thus provides an explanation for the various processes associated with precipitation variability changes between summer and winter.

Table 1
Correlations Between Convective Precipitation and Large-Scale Precipitation for the Different Climate States, Evaluated Separately for Winter and Summer

CO_2 concentration	Convective-large scale		Large scale-evaporation		Convective-evaporation		Convective-PMT	
	Winter	Summer	Winter	Summer	Winter	Summer	Winter	Summer
0.25x	0.64*	0.56*	0.06	0.05	0.37*	0.38*	0.64*	0.65*
0.5x	0.48*	0.53*	0.14**	−0.23*	0.76*	0.10**	0.29*	0.67*
Control	0.15*	0.60*	−0.12**	−0.32*	0.81*	0.01	0.03	0.73*
2x	−0.05	0.57*	−0.29*	−0.24*	0.82*	−0.06	0.00	0.73*
4x	−0.03	0.61*	−0.39*	−0.34*	0.76*	−0.10	0.09	0.79*

*$p < 0.01$. **$p < 0.05$).

However, it remains unclear why the changes in precipitation variability during summer (with respect to the control climate) are larger than the changes in mean summer precipitation. The correlation between PMT and precipitable water in the Arctic during summer is low across all climate states (not shown). This is due to both the abundance of moisture in summer and increased stability (compared to winter) over the open water inhibiting convective precipitation (Groves & Francis, 2002; Serreze & Etringer, 2003).

The low correlation between precipitable water (thermodynamical component of moisture transport) and PMT hints at an increased occurrence of more (intense) cyclones in warmer climates in summer (dynamical component of moisture transport). This is supported by several studies (Sorteberg & Walsh, 2008; Tilinina et al., 2013), which reported increased activity of summer cyclones over the last 50 years, during which the global (and Arctic) temperature has been increasing strongly. To provide an (indirect) indication of the prevalence of cyclones, the correlation between PMT and geostrophic wind speeds is shown in Figure 8 for the three warm climate states in summer.

Figure 8 shows that the correlation between PMT and the geostrophic wind speed increases toward warmer climates, especially over northern Eurasia. If the cyclonic activity becomes more intense in warmer climates, the efficiency (e.g., stronger upward motions) through which precipitation is formed increases (even though models diverge in their future projections). This is already observed in recent observations (Tilinina et al., 2013). In combination with the greater abundance of atmospheric moisture, the increased cyclonic activity likely leads to enhanced precipitation variability in summer.

Another source of precipitation variability in summer can be attributed to the AO. In winter, the correlation between the AO index and precipitation does not exhibit a clear pattern across the different climate states (the Arctic average correlations between the AO index and precipitation variability across different climate states are 0.12, 0.34, 0.54, 0.43, and 0.55, respectively). In summer, the correlation is fairly high for all climates and slightly increases toward warmer climates (the Arctic average correlations between the AO index and precipitation variability across different climate states are 0.56, 0.50, 0.61, 0.60, and 0.67, respectively). The regions of highest regression values are located near the Pacific side of the Arctic basin, the Canadian Archipelago, and West Greenland, and also, these values increase toward warmer climates in summer (Figure S4).

It can be concluded that Arctic precipitation variability during summer is higher than in winter because of (i) a greater abundance of atmospheric moisture, (ii) more intense cyclonic activity toward warmer climates, and (iii) a relatively weak counteracting relation between evaporation and PMT due to higher air temperatures in summer.

3.6. Caveats and Limitations

A limitation of this study is that the only difference between the five climates was the atmospheric CO_2 forcing that is applied; other components such as land cover (ice and vegetation) and other greenhouse gas concentrations and aerosols were kept at their current levels/distributions. While these simulations are therefore not realistic scenarios for past and future climates, this study aims at understanding the processes associated with Arctic variability and its dependence on climate states, rather than quantifying such changes in a realistic future scenario.

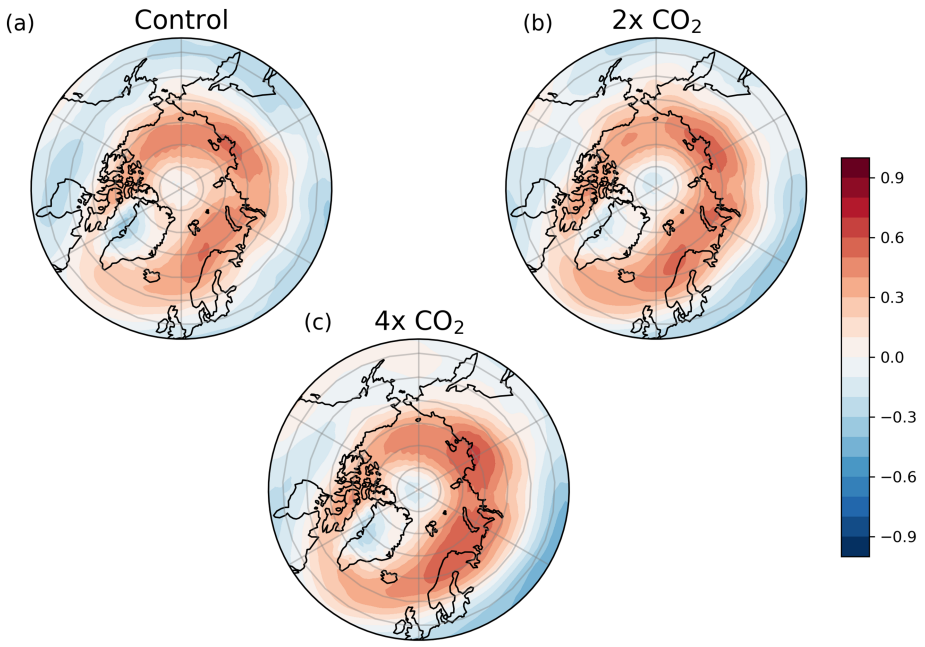

Figure 8. (a–c) Correlation between PMT and geostrophic wind speed at 500 hPa in summer for the three warm climate states.

Only one global climate model (EC-Earth) was used to assess long equilibrium climates, including warmer and colder than present climates. Using one model has the advantage of being able to focus in detail on process understanding but prohibits a discussion on uncertainties associated with model specifics (e.g., the resolution of EC-Earth is coarse relative to regional Arctic models, and cloud processes such as cloud water/ice composition and vertical transport of water vapor linked to inversion strength are relatively uncertain). A recent multimodel (CMIP5) study generally supports our results, that is, the increasing importance of evaporation for mean precipitation and the importance of the PMT in explaining projected increases in Arctic interannual precipitation variability toward warmer climates (Bintanja et al., 2020). We evaluated the simulated variability in Arctic precipitation for the current climate with reanalyses data and found largely good agreement.

Only monthly data could be used in this study. This time scale makes it more difficult to link variabilities to cyclonic activity because these have a time scale shorter than a month. Also, this makes it unfeasible to perform lead-lag analyses between evaporation within the Arctic and moisture transport across 70°N, because the transport of moisture from the extratropics toward the Arctic occurs on time scales shorter than 1 month. For further research, the use of daily time steps is recommended to study the causal relationship between Arctic evaporation and PMT.

The focus of this study has been on winter and summer. In spring and fall, however, the amount of precipitation influences sea ice melt (e.g., slower melt in years with more snowfall) and growth (e.g., postponed ice growth in years with enhanced rainfall). These spring/autumn changes might modulate important feedback mechanisms (such as increased surface evaporation triggering precipitation).

The time series were filtered with a Butterworth filter with a cutoff frequency of 0.1 year^{-1} to distinguish between interannual and decadal variabilities. We also explored the use of a rolling window to smooth the signals, but the Butterworth filter was found to possess a sharper cutoff (Figure S5).

Because we used the geostrophic wind at 500 hPa, it is difficult to separate the changes in moisture transport due to either the thermodynamical (q) or the dynamical (v) component. Inclusion of the wind components would enable differentiation between the mean, time deviation, and zonal deviations of the moisture transport (Boer et al., 2001; Dufour et al., 2016) and hence might provide new insights in the origin of precipitation variability, an endeavor to be investigated in a subsequent study.

4. Conclusion

Currently, little is known about the variability in the hydrological cycle of the Arctic region and especially about how it will change toward other climates. This study shows that precipitation variability increases toward warmer climates but does not directly scale with increases in the mean values. Wintertime precipitation variability is governed by both PMT and evaporation, which oppose each other as they both influence the vertical and meridional moisture gradients (e.g., if moisture transport increases, it reduces the vertical moisture gradient, which slows down the evaporation). The PMT is found to be dominant on interannual time scales, whereas the evaporation caused by sea surface temperature variability dominates on decadal time scales.

Our study illustrates the effects of changes in the climate on the means and the variability in Arctic precipitation (and related processes) and provides insights into the mechanisms that govern the changes in the hydrological cycle across different climate states and time scales. Our results, therefore, help to quantify and interpret changes in climate variability in the Arctic. To our knowledge, this is the first study discussing both the interannual and decadal variabilities in Arctic precipitation, in which a seasonal distinction is made. Because the mechanisms behind variability are found to be seasonal and climate state dependent, this study contributes to an improved understanding of all aspects of the Arctic hydrological cycle variability.

A better understanding of climate variability is important because long-term variability can obscure trends and because variability is associated with precipitation extremes (Pendergrass et al., 2017). Increased variability in the Arctic hydrological cycle also modifies surface runoff, which can alter changes in the salinity distribution of the ocean and thereby the oceanic circulation (Davies et al., 2014). On top of that, the changes in variability are especially enhanced in regions with amplified mean changes, for example, the margins of Greenland, leading to increased wet extremes that might impact society (e.g., water availability and infrastructure damage) (Vihma et al., 2016).

Acknowledgments
We would like to thank Willem Jan van de Berg (Utrecht University) and Rein Haarsma (KNMI) for their comments on an earlier version of the manuscript, Jesse Reusen (Delft University) and Joyce Mulder for their input during group meetings, and Michiel van den Broeke (Utrecht University) for discussions during the course of this research. We are grateful to the EC-Earth consortium for their contribution to the development of the Earth System Model EC-Earth (https://climexp.knmi.nl/selectfield_rea.cgi). We also thank the anonymous reviewers for their constructive comments and suggestions. The model and reanalyses data used in this study can be downloaded from https://data.knmi.nl/datasets/data_for_bogerdetal_jgrd_2019/1.0?q=arctic and https://climexp.knmi.nl/selectfield_rea.cgi, respectively.

References

AMAP (2012). Arctic climate issues 2011: Changes in Arctic snow, water, ice and permafrost. SWIPA 2011 Overview Report. Arctic Monitoring and Assessment Programme (AMAP), Oslo, Norway

Bengtsson, L., Hodges, K. I., Koumoutsaris, S., Zahn, M., & Keenlyside, N. (2011). The changing atmospheric water cycle in Polar Regions in a warmer climate. *Tellus Series A: Dynamic Meteorology and Oceanography*, *63*(5), 907–920.

Bintanja, R., & Selten, F. M. (2014). Future increases in Arctic precipitation linked to local evaporation and sea-ice retreat. *Nature*, *509*(7501), 479–482. https://doi.org/10.1038/nature13259

Bintanja, R., van der Wiel, K., van der Linden, E. C., Reusen, J., Bogerd, L., Krikken, F., & Selten, F. M. (2020). Strong future increases in Arctic precipitation variability linked to poleward moisture transport. *Science Advances*, *6*, eaax6869.

Boer, G. J. (2009). Changes in interannual variability and decadal potential predictability under global warming. *Journal of Climate*, *22*(11), 3098–3109.

Boer, G. J., Fourest, S., & Yu, B. (2001). The signature of the annular modes in the moisture budget. *Journal of Climate*, *14*(17), 3655–3665.

Davies, F. J., Renssen, H., & Goosse, H. (2014). The Arctic freshwater cycle during a naturally and an anthropogenically induced warm climate. *Climate Dynamics*, *42*(7–8), 2099–2112.

Dee, D. P., Uppala, S. M., Simmons, A. J., Berrisford, P., Poli, P., Kobayashi, S., et al. (2011). The ERA-Interim reanalysis: Configuration and performance of the data assimilation system. *Quarterly Journal of the Royal Meteorological Society*, *137*(656), 553–597. https://doi.org/10.1002/qj.828

Deser, C., Walsh, J. E., & Timlin, M. S. (2000). Arctic sea ice variability in the context of recent atmospheric circulation trends. *Journal of Climate*, *13*(3), 617–633.

Dufour, A., Zolina, O., & Gulev, S. K. (2016). Atmospheric moisture transport to the arctic: Assessment of reanalyses and analysis of transport components. *Journal of Climate*, *29*(14), 5061–5081.

Eastman, R., & Warren, S. G. (2010). Interannual variations of arctic cloud types in relation to sea ice. *Journal of Climate*, *23*(15), 4216–4232.

Francis, J. A., & Vavrus, S. J. (2015). Evidence for a wavier jet stream in response to rapid Arctic warming. *Environmental Research Letters*, *10*(1).

Gelaro, R., McCarty, W., Suárez, M. J., Todling, R., Molod, A., Takacs, L., et al. (2017). The modern-era retrospective analysis for research and applications, version 2 (MERRA-2). *Journal of Climate*, *30*(14), 5419–5454. https://doi.org/10.1175/JCLI-D-16-0758.1

Gillett, N. P. (2002). How linear is the Arctic Oscillation response to greenhouse gases? *Journal of Geophysical Research*, *107*(D3), 4022. https://doi.org/10.1029/2001JD000589

Groves, D. G., & Francis, J. A. (2002). Variability of the Arctic atmospheric moisture budget from TOVS satellite data. *Journal of Geophysical Research*, *107*(24), 4785. https://doi.org/10.1029/2002JD002285

Haarsma, R. J., Selten, F. M., & Drijfhout, S. S. (2015). Decelerating Atlantic meridional overturning circulation main cause of future west European summer atmospheric circulation changes. *Environmental Research Letters*, *10*(9).

Hassol, S. J., & Corell, R. W. (2006). Arctic climate impact assessment. In *Avoiding dangerous climate change* (Chap. 21). Cambridge, UK: Cambridge University Press.

Hawkins, E., & Sutton, R. (2009). The potential to narrow uncertainty in regional climate predictions. *Bulletin of the American Meteorological Society*, *90*(8), 1095–1108.

Hazeleger, W., Wang, X., Severijns, C., Ştefănescu, S., Bintanja, R., Sterl, A., et al. (2012). EC-Earth V2. 2: Description and validation of a new seamless Earth system prediction model. *Climate Dynamics*, *39*(11), 2611–2629. https://doi.org/10.1007/s00382-011-1228-5

Held, I. M., & Soden, B. J. (2006). Robust responses of the hydrological cycle to global warming. *Journal of Climate*, *19*(21), 5686–5699.

IPCC (2013). *Intergovernmental Panel on Climate Change Working Group I. Climate change 2013: The physical science basis. Long-term climate change: Projections, commitments and irreversibility* (pp. 1029–1136). New York: Cambridge University press.

Jakobson, E., & Vihma, T. (2010). Atmospheric moisture budget in the Arctic based on the ERA-40 reanalysis. *International Journal of Climatology*, *30*(14), 2175–2194.

Koenigk, T., & Brodeau, L. (2014). Ocean heat transport into the Arctic in the twentieth and twenty-first century in EC-Earth. *Climate Dynamics*, *42*(11–12), 3101–3120.

Koenigk, T., Brodeau, L., Graversen, R. G., Karlsson, J., Svensson, G., Tjernström, M., et al. (2013). Arctic climate change in 21st century CMIP5 simulations with EC-Earth. *Climate Dynamics*, *40*(11–12), 2719–2743. https://doi.org/10.1007/s00382-012-1505-y

Manabe, S., & Stouffer, R. J. (1980). Sensitivity of a global climate model to an increase of CO_2 concentration in the atmosphere. *Journal of Geophysical Research*, *85*(C10), 5529–5554.

Mernild, S. H., Hanna, E., Mcconnell, J. R., Sigl, M., Beckerman, A. P., Yde, J. C., et al. (2015). Greenland precipitation trends in a long-term instrumental climate context (1890-2012): Evaluation of coastal and ice core records. *International Journal of Climatology*, *35*(2), 303–320. https://doi.org/10.1002/joc.3986

Oshima, K., & Yamazaki, K. (2004). Seasonal variation of moisture transport in polar regions and the relation with annular modes*. *Polar Meteorology and Glaciology*, *18*, 30–53.

Pendergrass, A. G., Knutti, R., Lehner, F., Deser, C., & Sanderson, B. M. (2017). Precipitation variability increases in a warmer climate. *Scientific Reports*, *7*(1), 1–9.

Reusen, J., Van der Linden, E., & Bintanja, R. (2019). Differences between Arctic interannual and decadal variability across climate states. *Journal of Climate*, *32*(18), 6035–6050.

Rind, D., Perlwitz, J., & Lonergan, P. (2005). AO/NAO response to climate change: 1. Respective influences of stratospheric and tropospheric climate changes. *Journal of Geophysical Research*, *110*, D12107. https://doi.org/10.1029/2004JD005103.

Saha, S., Moorthi, S., Pan, H.-L., Wu, X., Wang, J., Nadiga, S., et al. (2010). The NCEP climate forecast system reanalysis. *Bulletin of the American Meteorological Society*, *91*(8), 1015–1058. https://doi.org/10.1175/2010BAMS3001.1

Schuenemann, K. C., & Cassano, J. J. (2010). Changes in synoptic weather patterns and Greenland precipitation in the 20th and 21st centuries: 2. Analysis of 21st century atmospheric changes using self-organizing maps. *Journal of Geophysical Research*, *115*, D05108. https://doi.org/10.1029/2009JD011706

Screen, J. A., Deser, C., Simmonds, I., & Tomas, R. (2014). Atmospheric impacts of Arctic sea-ice loss, 1979-2009: Separating forced change from atmospheric internal variability. *Climate Dynamics*, *43*(1–2), 333–344.

Screen, J. A., & Simmonds, I. (2010). The central role of diminishing sea ice in recent Arctic temperature amplification. *Nature*, *464*(7293), 1334–1337. https://doi.org/10.1038/nature09051

Serreze, M. C., & Etringer, A. J. (2003). Precipitation characteristics of the Eurasian Arctic drainage system. *International Journal of Climatology*, *23*(11), 1267–1291.

Serreze, M. C., & Francis, J. A. (2006). The Arctic amplification debate. *Climatic Change*, *76*(3–4), 241–264.

Serreze, M. C., & Hurst, C. M. (2000). Representation of mean arctic precipitation from NCEP-NCAR and ERA reanalyses. *Journal of Climate*, *13*(1), 198–201.

Sorteberg, A., & Walsh, J. E. (2008). Seasonal cyclone variability at 70°N and its impact on moisture transport into the Arctic. *Tellus, series A: Dynamic meteorology and oceanography*, *60*(A(3)), 570–586.

Sterl, A., Bintanja, R., Brodeau, L., Gleeson, E., Koenigk, T., Schmith, T., et al. (2012). A look at the ocean in the EC-Earth climate model. *Climate Dynamics*, *39*(11), 2631–2657.

Taylor, K. E., Stouffer, R. J., & Meehl, G. A. (2012). An overview of CMIP5 and the experiment design. *Bulletin of the American Meteorological Society*, *93*(4), 485–498.

Thompson, D. W. J., & Wallace, J. M. (1998). The Arctic oscillation signature in the wintertime geopotential height and temperature fields. *Geophysical Research Letters*, *25*(9), 1297–1300.

Tilinina, N., Gulev, S. K., Rudeva, I., & Koltermann, P. (2013). Comparing cyclone life cycle characteristics and their interannual variability in different reanalyses. *Journal of Climate*, *26*(17), 6419–6438.

Valcke, S., Caubel, A., Declat, D., & Terray, L. (2003). OASIS3 ocean atmosphere sea ice soil user's guide. Prisim Project Report, (2).

Van der Linden, E. C., Bintanja, R., & Hazeleger, W. (2017). Arctic decadal variability in a warming world. *Journal of Geophysical Research-Atmospheres*, *122*, 5677–5696. https://doi.org/10.1002/2016JD026058

Van der Linden, E. C., Bintanja, R., Hazeleger, W., & Graversen, R. G. (2016). Low-frequency variability of surface air temperature over the Barents Sea: Causes and mechanisms. *Climate Dynamics*, *47*(3–4), 1247–1262.

Van der Linden, E. C., Le Bars, D., Bintanja, R., & Hazeleger, W. (2019). Oceanic heat transport into the Arctic under high and low CO_2 forcing. *Climate Dynamics*, *53*(7-8), 4763–4780. https://doi.org/10.1007/s00382-019-04824-y

Vavrus, S., & Harrison, S. P. (2003). The impact of sea-ice dynamics on the Arctic climate system. *Climate Dynamics*, *20*(7–8), 741–757.

Vihma, T., Screen, J., Tjernström, M., Newton, B., Zhang, X., Popova, V., et al. (2016). The atmospheric role in the Arctic water cycle: A review on processes, past and future changes, and their impacts. *Journal of Geophysical Research: Biogeosciences*, *121*(3), 586–620.

Zhang, J., Lindsay, R., Schweiger, A., & Steele, M. (2013). The impact of an intense summer cyclone on 2012 Arctic sea ice retreat. *Geophysical Research Letters*, *40*, 720–726. https://doi.org/10.1002/grl.50190